ACS APPLIED MATERIALS & INTERFACES

Research Article

www.acsami.org

Gas Separation Membranes Derived from High-Performance Immiscible Polymer Blends Compatibilized with Small Molecules

Nimanka P. Panapitiya, Sumudu N. Wijenayake, Do D. Nguyen, Yu Huang, Inga H. Musselman, Kenneth J. Balkus, Jr., and John P. Ferraris*

The University of Texas at Dallas, Department of Chemistry and Biochemistry, 800 West Campbell Road, Richardson, Texas 75080, United States

Supporting Information

ABSTRACT: An immiscible polymer blend comprised of high-performance copolyimide 6FDA-DAM:DABA(3:2) (6FDD) and polybenzimidazole (PBI) was compatibilized using 2-methylimidazole (2-MI), a commercially available small molecule. Membranes were fabricated from blends of 6FDD:PBI (50:50) with and without 2-MI for H_2/CO_2 separations. The membranes demonstrated a matrix-droplet type microstructure as evident with scanning electron microscopy (SEM) imaging where 6FDD is the dispersed phase and PBI is the continuous phase. In addition, membranes with 2-MI demonstrated a uniform microstructure as observed by smaller and more uniformly dispersed 6FDD domains in contrast to 6FDD:PBI (50:50) blend membranes without 2-MI. This compatibilization effect of 2-MI was attributed to interfacial localization of 2-MI that lowers the interfacial energy similar to a surfactant. Upon the incorporation of 2-MI, the H_2/CO_2 selectivity improved remarkably, compared to the pure blend, and surpassed the Robeson's upper bound. To our knowledge, this is the first report of the use of a small molecule to compatibilize a high-performance immiscible polymer blend. This approach could afford a novel class of membranes in which immiscible polymer blends can be compatibilized in an economical and convenient fashion.

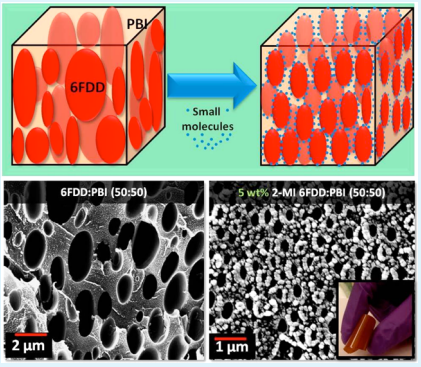

KEYWORDS: *immiscible polymer blends, compatibilizers, small molecules, gas separations, membrane microstructure*

INTRODUCTION

Membrane technology has become a promising alternative to conventional energy intensive gas separation methods and is used commercially for H_2 recovery, CO_2 recovery from natural gas, and on-site nitrogen production from air.[1−4] The selectivity/permeability trade-off of polymer-based membranes in gas separations, shown by Robeson,[5,6] has motivated researchers to develop membranes that surpass the upper bound. Despite the many efforts that have been made to exceed the upper bound, including the synthesis of new polymers,[7−11] cross-linking of the polymers,[12−14] fabrication of inorganic−organic composite materials (mixed-matrix membranes),[15−18] carbon molecular sieve membranes,[19−22] and use of polymer blends,[23] only a very few systems have emerged that exceed this now 2-decade old limit. While each of these approaches has its own advantages and disadvantages, there is still the need for novel materials with superior performances. However, the synthesis of novel materials is time-consuming and costly. Therefore, it would be beneficial to explore alternative approaches, such as the development of novel membrane microstructures and using blends of already known high-performance polymers.

Polymer blends have been used for various applications including photovoltaics,[24] light emitting diodes,[25] food packaging,[26] fuel cells,[27] and energy storage devices.[28] This approach has been attractive since it synergistically combines the superior properties of different polymers.[29] Also, blending is a less time-consuming and more cost-effective method compared to synthesizing new polymers. Because of these advantages, polymer blends have been used for membrane-based separations including pervaporation,[30] desalination,[31] and gas separations.[29] Enhancement in permeability and selectivity has been shown for *miscible* polymer blends, such as polyimides with polybenzimidazole (PBI),[32−34] sulfonated PEEK (SPEEK),[35] and poly(ether sulfone) (PES).[36] Even though the use of polymer blends is encouraging for gas separations, the limitation is their inherent immiscibility that occurs due to the unfavorable thermodynamics of mixing.[29] Nevertheless, membranes prepared from immiscible polymer blends have also been reported for gas separations.[37] Since the immiscibility of polymers lead to poor mechanical and gas separation properties, the enormous potential of blends to improve separation properties has yet to be realized. Therefore, by using the compatibilized immiscible polymer blends (CIPBs) described herein, this limitation can be lifted to allow the combination of a wide variety of polymers. Generally, copolymers[38] and nanomaterials[39,40] are used to compatibilize immiscible polymer blends to obtain uniform microstructures.

Received: June 9, 2015
Accepted: August 10, 2015
Published: August 10, 2015

DOI: 10.1021/acsami.5b04747
ACS Appl. Mater. Interfaces 2015, 7, 18618−18627

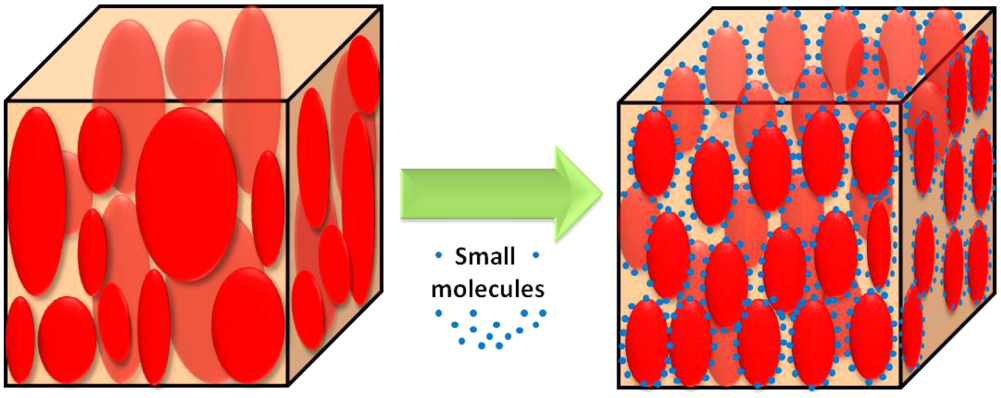

Figure 1. Illustration of proposed novel membrane microstructure in which a highly permeable polymer (red) is dispersed in a continuous, highly selective polymer (white) matrix.

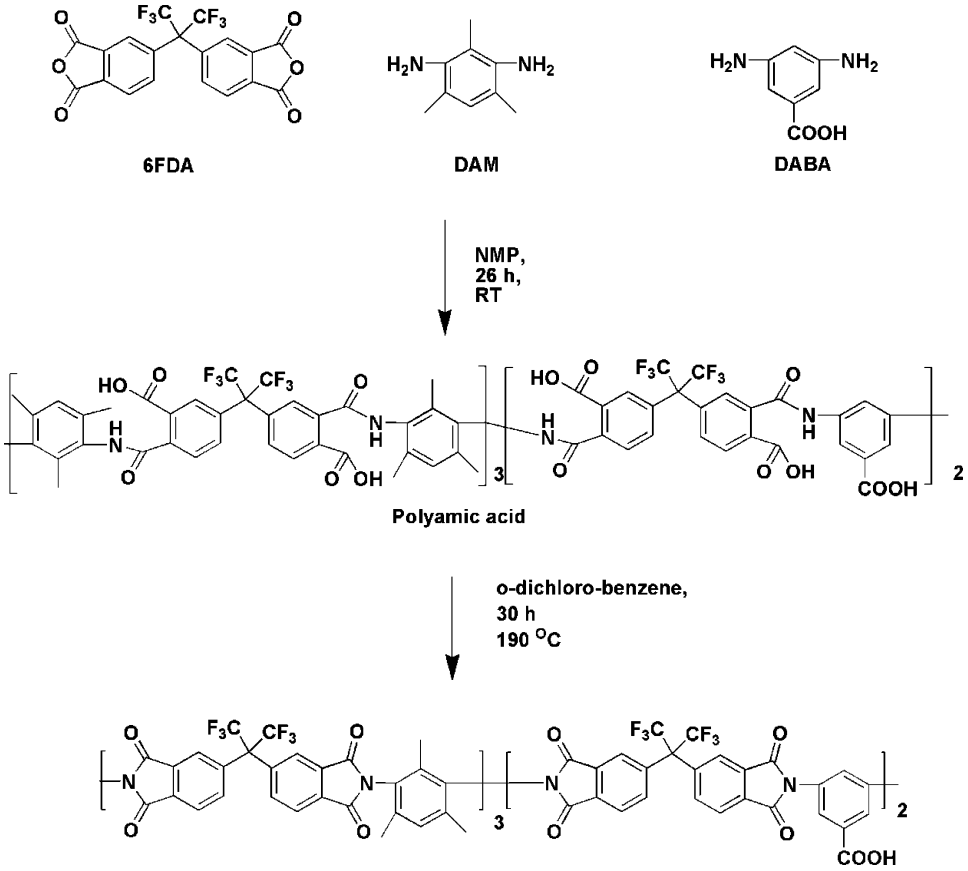

Figure 2. Synthesis procedure for 6FDA-DAM: DABA (3:2) copolyimide.

However, the synthesis of copolymers is tedious,[41] and applicability is limited to a single or a few blend compositions. Nanoparticles also need synthesis and sometimes chemical modifications.[42] Here, we report for the first time, the use of *small molecules* to compatibilize immiscible blends of PBI and a copolyimide (6FDD) to form membranes with a uniform and novel microstructure to improve gas separation performance. These small molecules are commercially available, inexpensive, and easy to use.

One important aspect of determining the performance of an immiscible polymer blend-based membrane is its morphology.[43] The matrix-droplet type morphology is advantageous for membrane transport since it can provide a large interfacial area to enhance flux. With this understanding, we report the fabrication of this novel class of membranes of an immiscible 6FDD and PBI blend stabilized by commercially available 2-methylimidazole (2-MI). 4,4-(Hexafluoroisopropylidene) diphthalic anhydride (6FDA)-based polyimides have high gas permeabilities due to their high free volume,[44] while PBI has high selectivity.[45] By combining both polymers, the resulting novel membrane microstructure contains thin, continuous ribbons in an otherwise noncontinuous polymer matrix. The highly permeable phase occupies most of the effective area/volume (dispersed phase) to achieve high flux (Figure 1), while the continuous phase is composed of PBI to ensure higher

DOI: 10.1021/acsami.5b04747
ACS Appl. Mater. Interfaces 2015, 7, 18618−18627

selectivity. The proposed work describes a new strategy to achieve the next generation gas separation membranes.

EXPERIMENTAL SECTION

Materials. All chemicals and solvents were used as received unless otherwise noted. Anhydrous 1-methyl-2-pyrrolidone (NMP, 99.8% purity) and 2-methylimidazole were purchased from Sigma-Aldrich. Anhydrous dimethylacetamide (DMAc, 99.8% purity) was purchased from EMD chemicals. 4,4-(Hexafluoroisopropylidene) diphthalic anhydride (6FDA, > 99% purity) was purchased from Akron Polymer Systems Inc. and was dried under vacuum at 150 °C prior to use. 2,4,6-Trimethyl-1,3-phenylenediamine (DAM, > 97% purity) was purchased from TCI America and purified further by vacuum sublimation. 3,5-Diaminobenzoic acid (DABA, 98% purity) was purchased from Sigma-Aldrich and was purified by recrystallization from water. Polybenzimidazole (PBI) was purchased from PBI Performance Products, Inc. (26 wt % in DMAc, 1.5% (w/w) LiCl, Mw ~ 30 000) and was used as received.

Synthesis of 6FDA-DAM:DABA (6FDD, 3:2 Molar Ratio) Polyimide. The synthesis of 6FDD (Figure 2) was carried out using thermal imidization (in NMP) following a published procedure.[46] The reaction was conducted under a nitrogen purge in a 100 mL three-neck flask equipped with a Dean−Stark apparatus and a condenser. In the first step, 2.00 g of 6FDA (4.502 mmol) in 8.5 mL of NMP was added dropwise to a solution of 0.274 g (1.808 mmol) DABA (3,5-diaminobenzoic acid) in 2.5 mL of NMP. (The monomer concentration in the flask was kept at ~20 wt %.) The mixture was stirred for 1 h at room temperature. Then, 0.406 g (2.70 mmol) of DAM (diaminomesitylene) monomer in 2.00 mL of NMP was added to the reaction flask and stirred at room temperature for 26 h to produce polyamic acid. Next, 1.00 mL of NMP and 5.00 mL of *o*-dichlorobenzene were added to the reaction mixture, which was then heated to 190 °C and maintained at this temperature with stirring for 30 h. Finally, the polymer solution was precipitated into 100 mL of 1:1 water/methanol, filtered, and washed with methanol. The resultant beige powder was dried under vacuum for 2 days at 120 °C. This method yielded 0.4 g of pale brown polymer (92% yield) with Mw of 170 000 and PDI of 2.3.

Membrane Fabrication. Separate solutions of ~2% (w/w) PBI and 6FDD were prepared in DMAc by stirring at 80 °C for 24 h followed by filtering through 0.45 μm syringe filters. In the preparation of polymer blends, solutions of 6FDD were always added to PBI solutions. The total polymer concentration of the final polymer mixture solution was ~2% (w/w). To induce phase separation as well as to concentrate the blend solution, excess DMAc was evaporated at 80 °C. The concentrated polymer solutions were then cast onto a glass substrate using a Sheen automatic applicator (1133N) equipped with a doctor blade. The membranes were initially dried using a heated casting table (50 °C for 12 h) under a N_2 flow. Finally, the membranes were peeled off from the glass substrate and annealed further under vacuum using a heating cycle of 80 °C for 24 h, 150 °C for 12 h, 200 °C for 12 h, and 250 °C for 24 h, followed by cooling to room temperature under vacuum.

The CIPB membranes were fabricated in the same way as the pure polymer blend membrane but with the addition of a 2-MI solution. The weight ratios of 5% and 9% [(weight of 2-MI/(total polymer weight + 2-MI weight)] 2-MI in DMAc were prepared separately and subjected to alternate stirring and sonication (15 min each) to ensure good dispersion. This cycle was repeated for 2 h. Then, one-third of the PBI solution was added to the dispersion. The resulting 2-MI polymer dispersion was stirred for 30 min and sonicated for another 30 min. This cycle was repeated twice. Then, the rest of the PBI was added and stirred at 80 °C for 12 h in a closed glass vial. After that, the 6FDD polymer solution was added dropwise to the 2-MI/PBI mixture and stirred further. Finally, excess DMAc was evaporated at 80 °C to obtain ~15 wt % solution. Casting, drying, and annealing of the CIPBMs were performed using the same protocols as for the polymer blends.

Characterization. *Characterization of 6FDD.* Molecular weight (M_w) was determined (M_w 170 000, PDI 2.3) on a gel permeation chromatography (Viscotek GPCmax, VE2001) system equipped with a Viscotek TDA 302 triple array detector and two ViscoGEL I-Series (I-MBHMW 3078, Viscotek) columns in series. Tetrahydrofuran (THF) at a flow rate of 1 mL/min was used as the eluent, and polystyrene standards (Polymer Laboratories) were used for calibration. The chromatograms were analyzed using OmniSEC Software, version 4.6.

Characterization of Membranes (SEM, TGA, FTIR, Mechanical Properties). Scanning electron microscope (SEM) images of membrane cross sections were acquired using a Zeiss SUPRA40 SEM with a field emission gun operating at 10 keV. Membrane cross sections for SEM imaging were prepared by freeze-fracturing the samples after immersion in liquid nitrogen. These samples were coated prior to imaging using a Denton Vacuum Desk II sputter coater equipped with a gold/palladium target. The thicknesses of the membranes used in permeability studies were also measured by SEM. Thermogravimetric analysis (TGA) was done under nitrogen using a PerkinElmer Pyris 1 TGA instrument at a heating rate of 10 °C/min. Fourier transform infrared (FTIR) spectra were acquired using a Nicolet 360 FTIR spectrophotometer with a single bounce attenuated total reflectance (ATR) accessory (diamond crystal). The mechanical properties of the membranes were tested at room temperature using a 584B Instron microtester.

Permeability Testing. Gas permeability testing was carried out using a custom built permeameter reported previously.[47] Pressure monitoring and valve actuations were controlled using LabVIEW 7.1 software (National Instruments). To acquire data, a 1 cm^2 piece of membrane was mounted inside a stainless steel cell, which separates the upstream side with a feed pressure of 2000 Torr from the downstream side, which is connected to a vacuum line (1 mTorr). Both upstream and downstream sides were evacuated for at least 6 h followed by a leak rate test before starting the experiments. Upstream and downstream pressures were recorded by pressure transducers. The steady state slope of the downstream pressure vs time was used to calculate permeability using the solution diffusion model.[48,49] Permeability was evaluated from the last 50% of the data in the steady state region. Ideal selectivities ($\alpha_{i/j}$) were calculated using the ratio of the permeabilities (P_i/P_j) of gases. Permeability testing was done for pure gases at 35 °C and 2000 Torr, and the permeability of a gas through an individual membrane was measured four times.

The Maxwell model can be used to predict the gas permeability properties of membranes having the phase separated matrix-droplet type morphology.[29,43] This model eq 1 was used to predict the gas permeability properties of the 6FDD:PBI (50:50) blend membrane.

$$P_{\text{eff}} = P_c\left[\frac{P_D + 2P_C - 2\phi_D(P_C - P_D)}{P_D + 2P_C + \phi_D(P_C - P_D)}\right] \quad (1)$$

P_{eff} is the effective permeability of the blend membrane, and P_C and P_D refer to the gas permeabilities of the continuous PBI phase and the dispersed 6FDD phase, respectively. The permeability data for 6FDD and PBI are listed in Table 2.

The volume fraction (ϕ_D) of 6FDD in the blend membranes was calculated using eq 2.

$$\phi_D = \frac{(m_D/\rho_D)}{(m_D/\rho_D) + (m_C/P_C)} \quad (2)$$

In the equation, m and ρ are mass and density, respectively. The reported density of PBI is 1.30 g cm^{-3},[50] and the reported density of 6FDD is 1.4 g cm^{-3}.[51] Using these data, the 6FDD volume fraction (ϕ_D) of 0.49 was derived for the 6FDD:PBI (50:50) blend membrane.

RESULTS AND DISCUSSION

Fabrication of the Membranes. Fabricated membranes were annealed at high temperatures to remove the DMAc solvent, following a temperature cycle ranging from 50 to 250 °C. The membranes were very flexible as shown in Figure 3.

DOI: 10.1021/acsami.5b04747
ACS Appl. Mater. Interfaces 2015, 7, 18618−18627

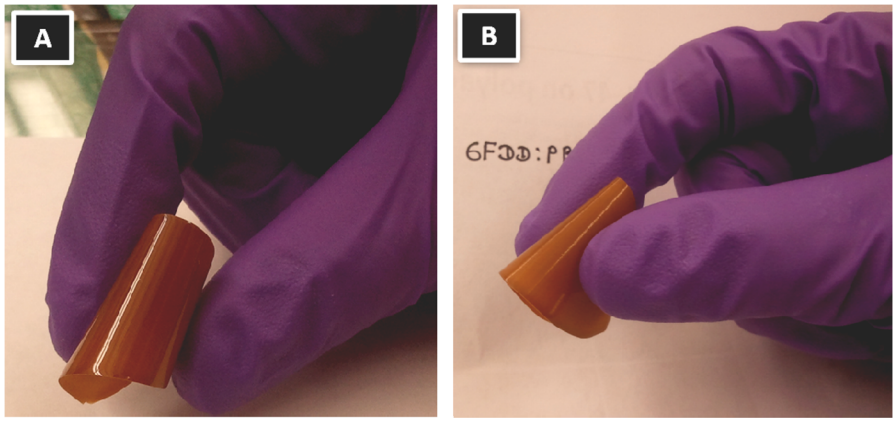

Figure 3. Optical images of 6FDD:PBI (50:50) membranes with (a) 5 wt % and (b) 9 wt % 2-MI.

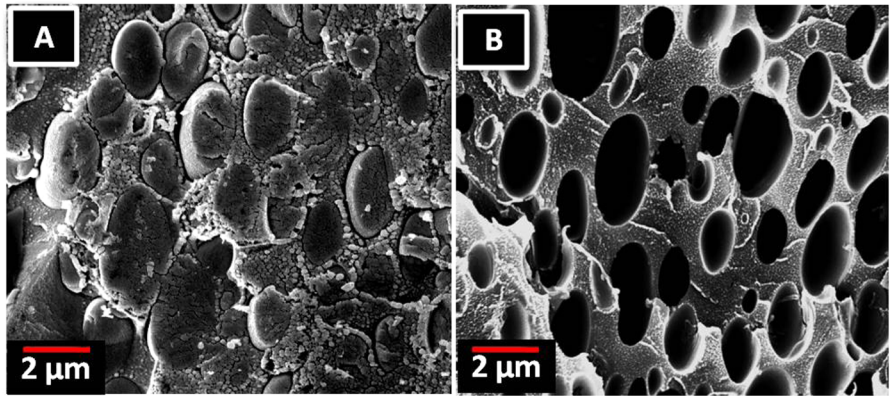

Figure 4. SEM images of 6FDD:PBI (50:50) membrane cross sections (A) before and (B) after selective THF extraction of 6FDD.

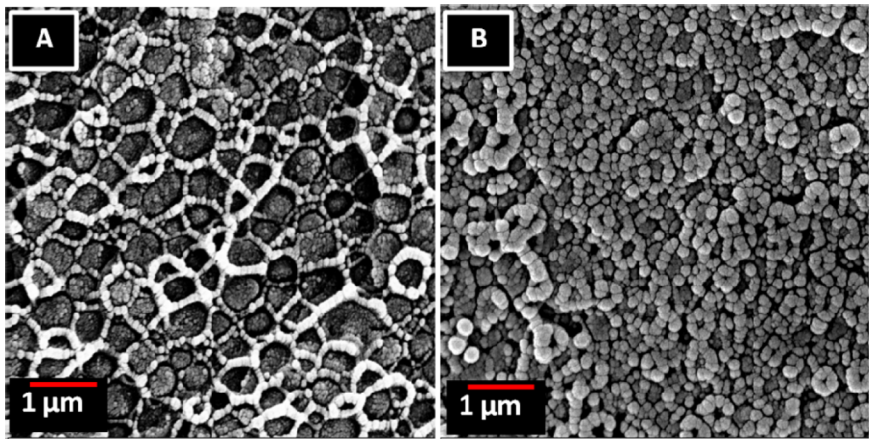

Figure 5. SEM images of 6FDD:PBI (50:50) membrane cross sections with (A) 5 wt % and (B) 9 wt % 2-MI.

Microstructure of the Blend Membranes. The microstructures of the blend membranes were observed by acquiring SEM images of the membrane cross sections. The identities of the dispersed and continuous phases of the 6FDD:PBI (50:50) membranes, shown in Figure 4A, were confirmed by subjecting the membrane to Soxhlet extraction using THF, which selectively removes the 6FDD phase. Figure 4B shows an SEM image of a 6FDD:PBI (50:50) THF-extracted membrane confirming that the dispersed phase is 6FDD and the continuous phase is PBI. This membrane microstructure has the desired matrix-droplet type morphology as predicted in the hypothesized model.

However, the size and the distribution of the dispersed phase domains are not uniform, and this microstructure is typical of an immiscible polymer blend. Surprisingly when 5 wt % of 2-MI was incorporated into the 6FDD:PBI (50:50) blend, the domain sizes of the 6FDD became smaller and more uniform (Figure 5A) compared to the pure polymer blend (Figure 4A). At an increased 2-MI loading of 9 wt %, the domain size of the dispersed phase was further decreased (Figure 5B). This observation is similar to what we recently reported for the ZIF-8 6FDD:PBI (50:50) membrane system.[52]

This effect of domain size reduction with increased 2-MI content can be further illustrated by the histograms in Figure 6.

DOI: 10.1021/acsami.5b04747
ACS Appl. Mater. Interfaces 2015, 7, 18618−18627

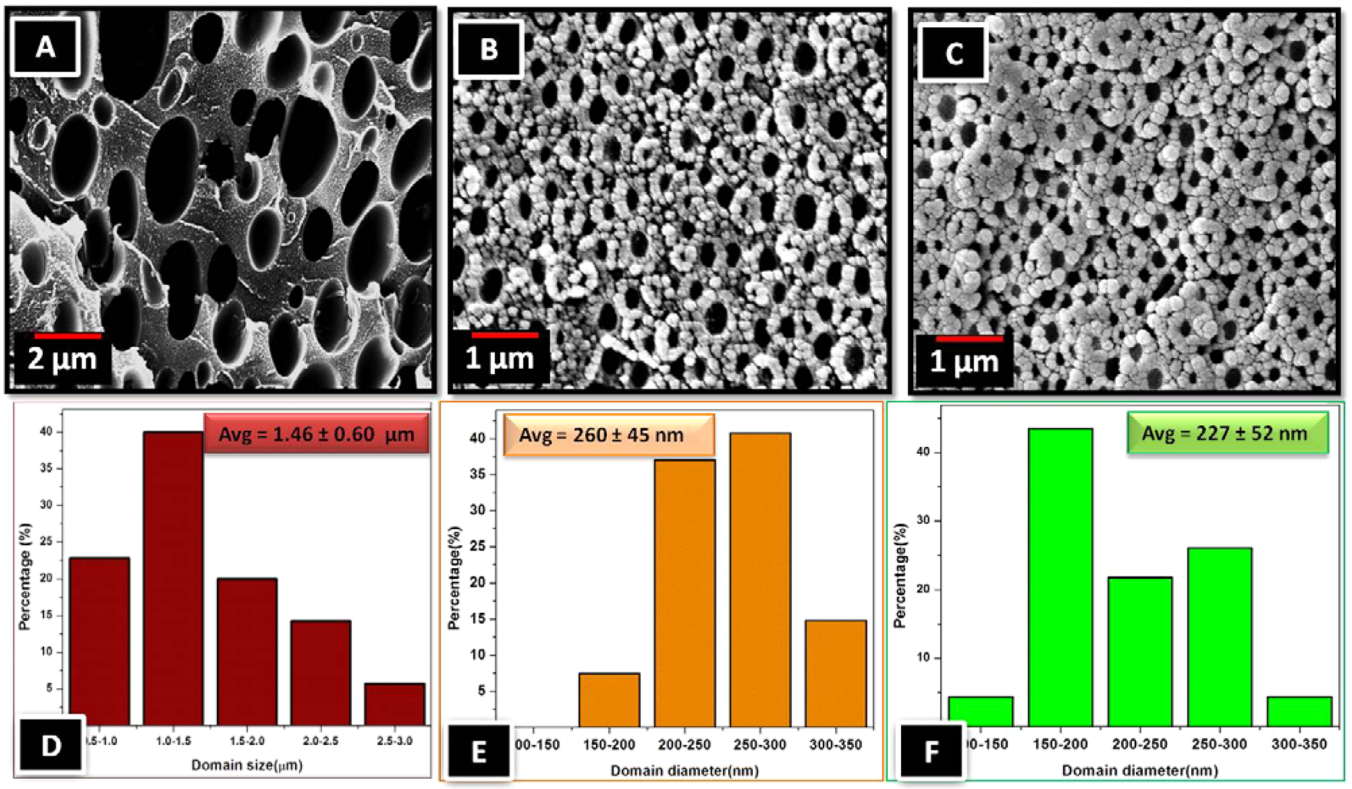

Figure 6. SEM images (A−C) and histograms (D−F) of the 6FDD-extracted 6FDD:PBI (50:50) membranes containing (A,D) 0 wt %, (B,E) 5 wt %, and (C,F) 9 wt % 2-MI.

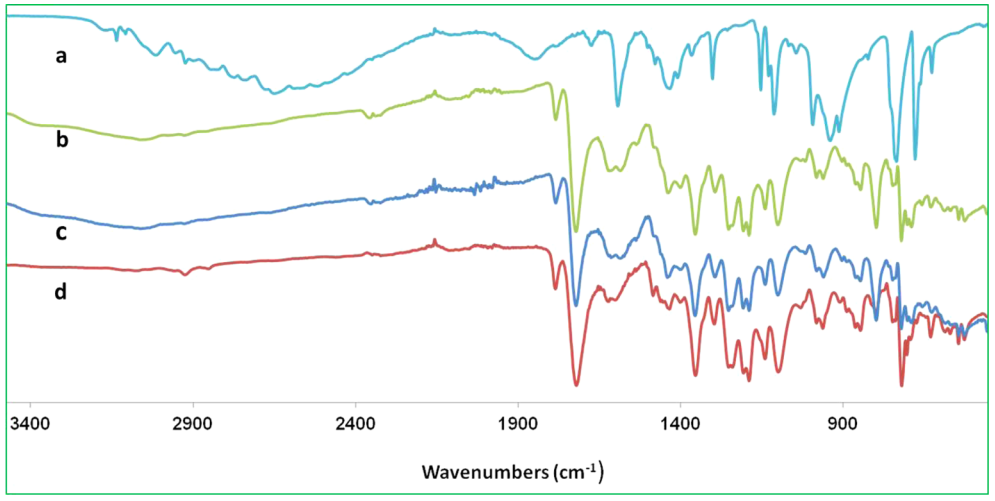

Figure 7. ATR-FTIR spectra of (a) 2-MI and of 6FDD:PBI (50:50) blend membranes with (b) 9 wt %, (c) 5 wt %, and (d) 0 wt % of 2-MI.

The average domain size of the dispersed phase is large (1.46 ± 0.60 μm) and shows a wide distribution in the 6FDD:PBI (50:50) blend (Figure 6 A,D) without 2-MI addition. However, with only 5 wt % 2-MI added to the same blend (Figure 6 B,E), the average domain size decreased to 260 ± 45 nm. It is important to note that not only did the dispersed domains become smaller but they also became more uniform in size after the incorporation of 2-MI. As the 2-MI loading was further increased to 9 wt % (Figure 6C,F), the average domain size of the 6FDD phase became even smaller (227 ± 52 nm), a modest reduction compared to that of the 5 wt % 2-MI, but a large reduction compared to the 6FDD:PBI (50:50) blend. This result indicates that as the 2-MI loading increases, the domain size of the dispersed phase becomes smaller and more uniform compared to that of the pure polymer blend.

ATR-FTIR and TGA Analysis of Blend Membranes. ATR-FTIR spectroscopy was performed in order to confirm the presence of individual components in the blend membranes and also to investigate if any major chemical change has occurred during the membrane fabrication process. First, ATR-FTIR spectroscopic analysis was performed on pure polymers and 6FDD:PBI (50:50) blends (Figure S1). These spectra suggest the presence of both polymers and the absence of major chemical changes in the 6FDD:PBI (50:50) blend

DOI: 10.1021/acsami.5b04747
ACS Appl. Mater. Interfaces 2015, 7, 18618−18627

compared to the pure polymers. Next, the membranes with 2-MI were compared with the 6FDD:PBI (50:50) membrane (Figure 7).

2-MI shows characteristic vibrations at 780 cm^{-1}(−N−H waging), 1110 cm^{-1} (C−N stretching), 1850 cm^{-1} (imidazole ring vibration absorption), 2500−3200 cm^{-1} (C−H stretch in imidazole ring), and 3470 cm^{-1} (−N−H stretch).[53] However, the −NH absorption at 3470 cm^{-1} was not observed, which could be due to the intermolecular H-bonding. As shown in Figure 7, all of the membranes fabricated with 2-MI show a spectrum similar to that of the pure 6FDD:PBI (50:50) membrane. Here also, the characteristic peaks of both PBI and 6FDD polymers were present in the membranes without any major shifts. Furthermore, none of the peaks corresponding to 2-MI were found in any of the blend membranes. This could be due to the evaporation of 2-MI under vacuum during the annealing process. However, to confirm the absence of the 2-MI in the membranes, a TGA experiment was conducted with a 6FDD:PBI (50:50) membrane containing an initial loading of 9 wt % 2-MI and another without 2-MI (Figure S2). The TGA plot confirmed that 2-MI is not present in the membrane after annealing. Also, the ATR-FTIR results suggest that chemical functionalities have not changed due to the membrane fabrication procedure, which includes a phase transition of 2-MI (Figure 7).

Compatibilization Shown by the 2-MI. Compatibilization of immiscible polymer blends has been achieved utilizing different materials including copolymers and nanomaterials.[38−40] In copolymer controlled compatibilizers, the copolymer is localized at the interface, which lowers the interfacial tension. Generally, the copolymers are made of subunits of both polymers, and thus, they can migrate and localize at the interface. Nanoparticles have also been employed as compatibilizers and some of them have been grafted to polymer chains in order to be compatible with one polymer phase.[42] In addition to these materials, nanomaterials such as graphene oxide has been used as a compatibilizer due to its amphiphilic nature, which also allows it to localize at the interface.[54] Wu and co-workers have reported that graphene oxide sheets undergo H-bonding with polar polyimide polymers while forming strong hydrophobic interactions with polyphenylene oxide.[54] Similarly, 2-MI also contains an aromatic region which could possibly form hydrophobic interactions, while polar −NH and imine functionalities can form H-bonding.

To investigate these effects, membranes were fabricated incorporating 33.3 wt % 2-MI separately into 6FDD and PBI. Both membranes were annealed for 5 days at 100 °C, which is lower than the melting temperature of 2-MI. The resulting membranes were analyzed with TGA and ATR-FTIR. The weight loss from the 200 to 400 °C region is attributed to the removal of 2-MI. (Figures S3 and S4). The melting point of 2-MI is 142−143 °C, while the boiling point is 267−268 °C. This weight loss in both TGA plots confirmed the presence of 2-MI in the membranes. Also, the lack of weight loss up to 200 °C confirmed that the membranes were free of DMAc. After confirming the presence of 2-MI, ATR-FTIR analysis of the membranes was performed to investigate the potential chemical interactions between the polymers and 2-MI. However, significant peak shifts in the regions of interest were not observed in the PBI membrane loaded with 33.3 wt % 2-MI (Figure S5). The −C−H stretching vibration region of the 2-MI was not present in the 33.3 wt % 2-MI in the PBI membrane, which could be due to partial overlap with the −C−H stretching absorption region of PBI. This result suggests that there are no strong chemical interactions between 2-MI and PBI. However, since 2-MI has an imidazole moiety similar to PBI, it is possible that the 2-MI packs well within the polymer chains. Therefore, even though ATR-FTIR analysis would not confirm the presence of strong chemical interactions, it is possible that hydrophobic interactions exist especially in the overlapping regions.

The comparison of ATR-FTIR spectra of the membrane containing 33.3 wt % 2-MI in 6FDD with 2-MI and pure 6FDD reveals that most of the vibrations correspond to 2-MI overlap with that of the blend membrane (Figure 8). However, the

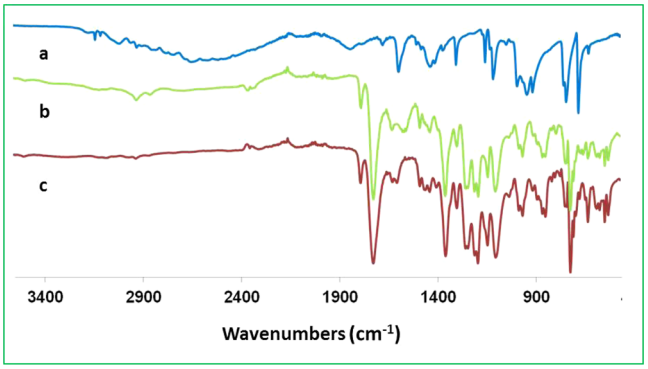

Figure 8. ATR-FTIR spectra of (a) 2-MI and 6FDD with (b) 33.3 wt % and (c) 0 wt % 2-MI.

−C═N stretching vibration that appears at ∼1593 cm^{-1} in 2-MI is more red-shifted in the blend membrane. It has been reported previously that the −OH functionalities are capable of forming H-bonds with imine N.[55]

Therefore, a close analysis was performed on the 1200−1900 cm^{-1} region where the −C═N stretch from 2-MI appears (Figure 9) and the 2500−3500 cm^{-1} region that corresponds to

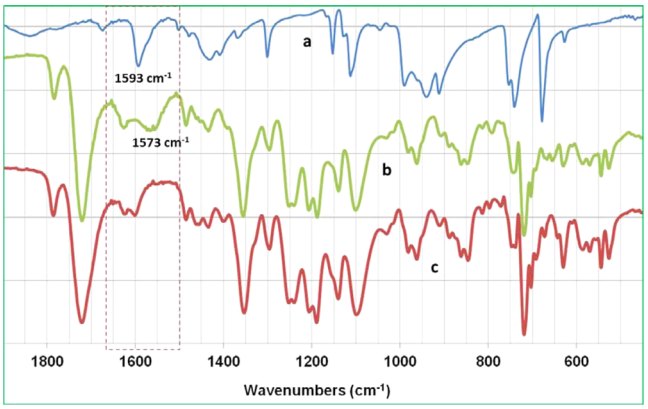

Figure 9. ATR-FTIR spectra (in the 600−1900 cm^{-1} region) of (a) 2-MI and 6FDD (b) with and (c) without 2-MI.

the −OH stretch due to the −COOH group of the DABA moiety of 6FDD (Figure 10). As shown in the Figure 9, a ∼20 cm^{-1} red shift in the imine stretching was observed, suggesting a clear alteration to the original bond. To confirm this effect further, the −OH stretching absorption was also closely examined. In pure 6FDD, a weak broad band appears between 3200 and 3400 cm^{-1} which is assigned to the −OH stretching

DOI: 10.1021/acsami.5b04747
ACS Appl. Mater. Interfaces 2015, 7, 18618−18627

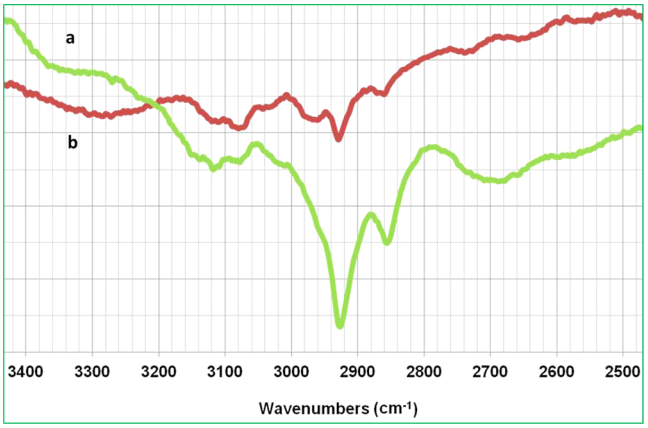

Figure 10. ATR-FTIR spectra of 6FDD (a) without and (b) with 2-MI.

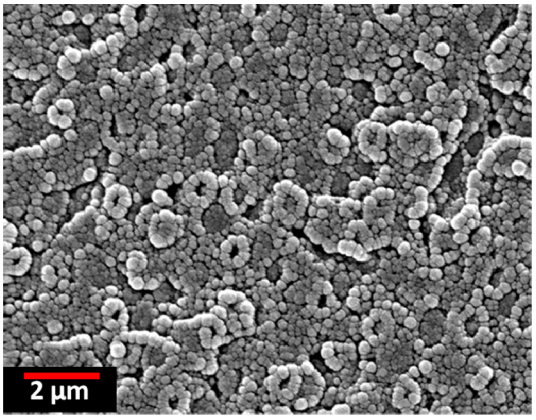

Figure 11. SEM image of a cross-section of a 9 wt % 2-MI 6FDD:PBI (50:50) membrane prepared using a modified procedure.

vibration (Figure 10b).[12] However, when 2-MI is incorporated into 6FDD, the −OH stretching absorption no longer appears in the spectrum (Figure 10a), suggesting possible interactions with 2-MI and, most probably, H-bonding between the −OH and imine functionalities, similar to previous reports.[55]

Since 2-MI can potentially form hydrophobic and $\pi-\pi$ interactions with PBI and H-bonds with 6FDD, it is possible for 2-MI to localize at the interface during the phase separation of the polymers, similar to a surfactant. However, one can envision that 2-MI can be in either the 6FDD or PBI phase. If 2-MI localizes in the 6FDD domains, the uniform morphology of the dispersed phase would not be observed because there would be no restriction to the phase coarsening of the dispersed phase to lower the interfacial tension. Therefore, if 2-MI localizes in the 6FDD domains, a microstructure similar to the pure 6FDD:PBI (50:50) blend would be observed (see Figure 4a). Localization of the nanoparticles in the continuous phase can also lead to uniform, dispersed domain structures since, in such an instance, the nanoparticles can act as a physical barrier for coalescence. However, with its lower surface area as compared to a nanoparticle, 2-MI may not be efficient in restricting coalescence. Therefore, 2-MI should localize *at* the interface, similar to a surfactant, minimizing interfacial tension between the polymer phases. To further support the argument, another membrane was fabricated by slightly modifying the procedure. In the prior method, 2-MI was added to PBI and subjected to prolonged stirring and sonication before adding 6FDD. In the modified procedure, 2-MI was first added to 6FDD and subjected to stirring and sonication and then PBI was added. After that, the membrane was cast following the same procedure. The resulting membrane microstructure was investigated using SEM and is shown in Figure 11. Surprisingly, similar to the other membranes containing 2-MI, this membrane contains a microstructure consisting of uniform 6FDD domains. If 2-MI localizes in the 6FDD phase by interacting with the imine groups, a uniform size distribution of 6FDD would not be observed since there would be no restriction for phase coarsening. Therefore, 2-MI has to migrate from the 6FDD phase to either the interface or the PBI phase in order to obtain such a morphology. Considering the ability of 2-MI to potentially form interactions with PBI as well, it is likely that it localizes at the interface, minimizing the overall interfacial energy of the system.

Polybenzimidazole (PBI) and 6FDA-based polyimides are high performance polymers having a high tensile strength and high elastic modulus compared to general purpose plastics such as polypropylene (PP) and low-density polyethylene (LDPE) (Table 1).

Table 1. Mechanical Properties of the Membrane Materials

material	tensile strength (MPa)	Young's modulus (GPa)
6FDD	44.3	2.3
PBI	160.0	1.9
6FDD-PBI	73.9	2.7
5 wt % 2-MI/6FDD:PBI (50:50)	86.6	3.1
9 wt % 2-MI/6FDD:PBI (50:50)	115.4	3.5
LDPE[56]	16.6	0.286
PP[56]	26.1	0.519

Compared to 6FDD, PBI has a higher tensile strength, which can be attributed to the closely packed aromatized structure of PBI. PBI is also known to be a strong and very hard polymer. Mechanical properties of the immiscible polymer blends depend on the morphology[57] and mechanical properties of the individual components. The tensile strength of the 6FDD:PBI (50:50) was less than half of pure PBI's as a result of the uncontrollable phase separation which causes the domain size of the dispersed phase to be large and nonuniform. Even though the continuous phase is PBI, which has the higher mechanical strength, the applied stress is not evenly transferred through the membrane. This happens due to both relatively lower mechanical strength of 6FDD and poor interfacial adhesion between the polymers. Similar observations have been reported before by Ma and co-workers in the preparation of starch/polylactic acid blends.[58] They further reported that as the domain size of the dispersed phase is decreased, the tensile strength of the blend is improved. A similar trend is observed in our system as the 6FDD domain size becomes smaller and more uniform, with 9 wt % 2-MI loading, the tensile strength increased ∼56% compared to the uncompatibilized blend, although it still does not reach that of pure PBI. Wu and co-workers have reported a remarkable increase in the mechanical strength of immiscible polyamide/polyphenylene (PPO) blends compatibilized with graphene oxide sheets (GOS), which they attributed to the high mechanical strength of GOS itself as well as the improved dispersion of PPO.[54] In contrast, when copolymers were used as compatibilizers for the same

DOI: 10.1021/acsami.5b04747
ACS Appl. Mater. Interfaces 2015, 7, 18618−18627

blend, the mechanical strength decreased as the copolymer content increased as a result of the "soft" nature of the copolymer.[59] The small molecule compatibilizers used in our work do not belong to either of these categories and would not be expected to impart any significant enhancements to the mechanical properties by themselves (as is the case for GOS), neither did the tensile strength decrease due to "soft" mechanical properties of the 2-MI. Hence we attribute the improvement in mechanical properties to the restricted phase separation of the small and uniform domains of 6FDD within a strong PBI matrix. 6FDD and PBI membranes demonstrate Young's moduli of 2.3 and 1.9, respectively, and compared to LDPE and PP, both 6FDD and PBI are stiff. An overall ~30% improvement of modulus is observed as the 2-MI loading reaches 9 wt %, compared to that of the pure blend. The smaller and more uniform dispersed phase domains in the compatibilized blends allow for more efficient energy transfer between the two phases.

Gas Permeability Properties. 6FDD is a glassy polyimide having high gas permeability with relatively low H_2/CO_2 selectivity (Table 2). PBI has higher selectivity values for H_2 separations but low H_2 permeability. A ~6-fold increase in H_2 permeability was obtained in the 6FDD:PBI (50:50) blend compared to pure PBI. Gas permeability properties calculated using the Maxwell model can be used to further explain the experimental results. As listed in Table 2, the predicted H_2/CO_2 selectivity of a 6FDD:PBI (50:50) membrane (calculated from P_{eff}) closely correlates with the experimental data. However, the measured permeabilities of H_2 and CO_2 are both slightly higher than the predicted values. Higher measured gas permeabilities can be attributed to the extra free volume created as a result of uncontrollable phase separation. However, the selectivity remains the same since the adsorbed gases pass through the continuous, highly selective PBI phase, as expected in the hypothesis. More importantly, when the membranes were compatibilized with 5 wt % 2-MI, both H_2 and CO_2 gas permeabilities decreased and became closer to the predicted values of 6FDD:PBI (50:50), with the selectivity remaining the same. This could be due to the compatibilization effect of 2-MI.

Then, as the 2-MI loading was further increased to 9 wt %, the H_2/CO_2 selectivity increased by ~250% as compared to the 6FDD:PBI (50:50) blend. This result indicates that the incorporation of 2-MI enhances the selectivity significantly in addition to compatibilizing the polymer blend. It is also important to note that the gas permeabilities decreased with increasing 2-MI loading (Figure 12). At 9 wt % loading of 2-MI, the CO_2 permeability decreased significantly (86%) compared to H_2 (47%), which accounts for the high H_2/CO_2 selectivity of 40 (Table 2). 2-MI undergoes a phase transition during the membrane annealing procedure in which it melts at 142−143 °C and boils at 267−268 °C.[60] Even though the highest annealing temperature is 250 °C, due to the presence of vacuum, 2-MI has been removed from the membranes as indicated by the TGA data (Figure S2). During this evaporation process, it is possible that 2-MI creates unique gas transport pathways that are more selective for H_2 transport over CO_2. Also, since 2-MI is localized at the polymer−polymer interface during the melting process, it is possible that this interface contains a residual amount of 2-MI that also contributes to lower the permeabilities of the gases. This increase in H_2/CO_2 selectivity results in gas permeability properties that surpass the Robeson upper bound for H_2/CO_2 separations (Figure 13).

Table 2. Gas Permeability[a] Properties of the Membranes

membrane	P-H_2	P-CO_2	α-H_2/CO_2
6FDD:PBI (50:50)	7.54 ± 0.66	0.73 ± 0.12	10.3 ± 1.1
6FDD:PBI (50:50)[b]	4.11	0.39	10.5
5 wt % 2-MI 6FDD:PBI (50:50)	5.80 ± 0.12	0.51 ± 0.07	11.3 ± 1.4
9 wt % 2-MI 6FDD:PBI (50:50)	4.04 ± 0.05	0.10 ± 0.02	40.4 ± 6.1
6FDD	100.00	52.60	1.9
PBI	1.11 ± 0.03	0.10 ± 0.01	11.1 ± 1.1

[a]Ideal gas permeability measured in Barrers at 2000 Torr and 35 °C. [b]Calculated using the Maxwell model.

CONCLUSIONS

High performance 6FDD/PBI blend membranes incorporating 2-MI were successfully fabricated and characterized, and gas permeability performances were determined. These membranes demonstrated a matrix-droplet type microstructure in which 6FDD is the dispersed phase and PBI is the continuous phase. Because of the incorporation of 2-MI, the membrane morphology became more uniform indicating a better compatibility between the polymers. This compatibilization effect of 2-MI was attributed to interfacial localization of 2-MI, which lowered the interfacial tension similar to a surfactant.

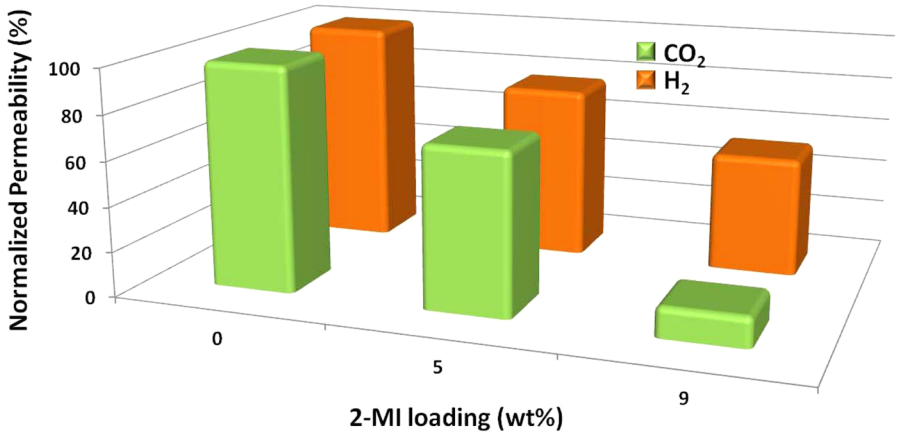

Figure 12. Normalized gas permeability versus 2-MI loading.

DOI: 10.1021/acsami.5b04747
ACS Appl. Mater. Interfaces 2015, 7, 18618−18627

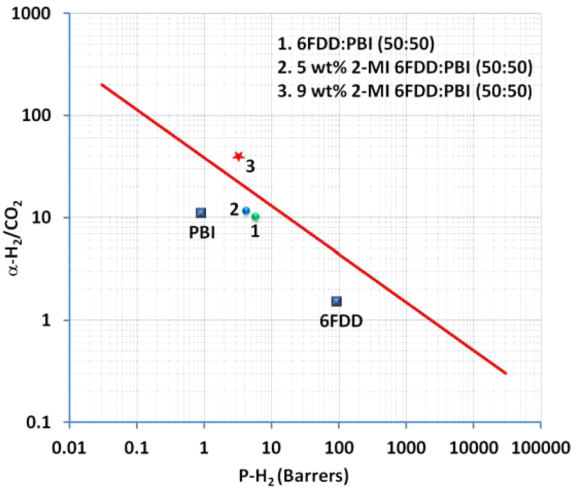

Figure 13. Gas separation properties of 6FDD:PBI blends depicted in a Robeson plot.

The mechanical properties of the blend membranes improved as a result of the compatibilization. To our knowledge, this is the first report of the use of a small molecule to compatibilize an immiscible polymer blend. The gas separation properties of the blend improved with the incorporation of 2-MI, surpassing the Robeson's upper bound. This work will open up new opportunities for blend-based membranes, where immiscible polymer blends can now be compatibilized in a cost-effective and convenient manner, resulting in superior separation performances.

■ ASSOCIATED CONTENT

Supporting Information

The Supporting Information is available free of charge on the ACS Publications website at DOI: 10.1021/acsami.5b04747.

ATR-FTIR spectra and TGA plots (PDF)

■ AUTHOR INFORMATION

Corresponding Author

*E-mail: ferraris@utdallas.edu.

Funding

The authors thank the National Science Foundation (CBET Grant 1403950 and Grant CHE-1126177 [for Bruker AVANCE III 500 NMR]) for the financial support provided for this research.

Notes

The authors declare no competing financial interest.

■ ACKNOWLEDGMENTS

The technical assistance of Dr. Winston Layne and Dr. Edson Perez is gratefully acknowledged.

■ REFERENCES

(1) Bernardo, P.; Drioli, E.; Golemme, G. Membrane Gas Separation: A Review/State of the Art. *Ind. Eng. Chem. Res.* **2009**, *48*, 4638−63.
(2) Baker, R. W.; Lokhandwala, K. Natural Gas Processing With Membranes: An Overview. *Ind. Eng. Chem. Res.* **2008**, *47*, 2109−21.
(3) Baker, R. W. Future Directions of Membrane Gas Separation Technology. *Ind. Eng. Chem. Res.* **2002**, *41*, 1393−411.
(4) Ma, X.; Swaidan, R.; Teng, B.; Tan, H.; Salinas, O.; Litwiller, E.; Han, Y.; Pinnau, I. Carbon Molecular Sieve Gas Separation Membranes Based on an Intrinsically Microporous Polyimide Precursor. *Carbon* **2013**, *62*, 88−96.
(5) Robeson, L. M. The Upper Bound Revisited. *J. Membr. Sci.* **2008**, *320*, 390−400.
(6) Robeson, L. M. Correlation of Separation Factor Versus Permeability for Polymeric Membranes. *J. Membr. Sci.* **1991**, *62*, 165−185.
(7) Sakaguchi, T.; Shiotsuki, M.; Sanda, F.; Freeman, B. D.; Masuda, T. Synthesis and Properties of F-Containing Poly(diphenylacetylene) Membranes. *Macromolecules* **2005**, *38*, 8327−8332.
(8) Lively, R. P.; Dose, M. E.; Xu, L.; Vaughn, J. T.; Johnson, J. R.; Thompson, J. A.; Zhang, K.; Lydon, M. E.; Lee, J. S.; Liu, L.; Hu, Z.; Karvan, O. U.; Realff, M. J.; Koros, W. J. A High-Flux Polyimide Hollow Fiber Membrane to Minimize Footprint and Energy Penalty for CO_2 Recovery From Flue Gas. *J. Membr. Sci.* **2012**, *423−424*, 302−313.
(9) Sanders, D. F.; Smith, Z. P.; Ribeiro, C. U. P., Jr; Guo, R.; McGrath, J. E.; Paul, D. R.; Freeman, B. D. Gas Permeability, Diffusivity, and Free Volume Of Thermally Rearranged Polymers Based on 3,3′-Dihydroxy-4,4′-Diamino-Biphenyl (HAB) and 2,2-bis-(3,4-dicarboxyphenyl) Hexafluoropropane Dianhydride (6FDA). *J. Membr. Sci.* **2012**, *409−410*, 232−241.
(10) Park, H. B.; Jung, C. H.; Lee, Y. M.; Hill, A. J.; Pas, S. J.; Mudie, S. T.; Van Wagner, E.; Freeman, B. D.; Cookson, D. J. Polymers with Cavities Tuned for Fast Selective Transport of Small Molecules and Ions. *Science* **2007**, *318*, 254−258.
(11) Park, H. B.; Jung, C. H.; Lee, Y. M.; Hill, A. J.; Pas, S. J.; Mudie, S. T.; Van Wagner, E.; Freeman, B. D.; Cookson, D. J. Polymers with Cavities Tuned for Fast Selective Transport of Small Molecules and Ions. *Science* **2007**, *318*, 254−258.
(12) Qiu, W.; Chen, C. C.; Xu, L.; Cui, L.; Paul, D. R.; Koros, W. J. Sub-Tg Cross-Linking of a Polyimide Membrane for Enhanced CO_2 Plasticization Resistance for Natural Gas Separation. *Macromolecules* **2011**, *44*, 6046−6056.
(13) Ribeiro, C. U. P., Jr; Freeman, B. D.; Paul, D. R. Pure- and Mixed-Gas Carbon Dioxide/Ethane Permeability and Diffusivity in a Cross-Linked Poly(ethylene oxide) Copolymer. *J. Membr. Sci.* **2011**, *377*, 110−123.
(14) Wijenayake, S. N.; Panapitiya, N. P.; Versteeg, S. H.; Nguyen, C. N.; Goel, S.; Balkus, K. J.; Musselman, I. H.; Ferraris, J. P. Surface Cross-Linking of ZIF-8/Polyimide Mixed-Matrix Membranes (MMMs) for Gas Separation. *Ind. Eng. Chem. Res.* **2013**, *52*, 6991−7001.
(15) Ordoñez, M. J. C.; Balkus, K. J., Jr.; Ferraris, J. P.; Musselman, I. H. Molecular Sieving Realized with ZIF-8/Matrimid Mixed-Matrix Membranes. *J. Membr. Sci.* **2010**, *361*, 28−37.
(16) Bae, T. H.; Lee, J. S.; Qiu, W.; Koros, W. J.; Jones, C. W.; Nair, S. A High-Performance Gas-Separation Membrane Containing Submicrometer-Sized Metal−Organic Framework Crystals. *Angew. Chem., Int. Ed.* **2010**, *49*, 9863−9866.
(17) Perez, E. V.; Balkus, K. J., Jr.; Ferraris, J. P.; Musselman, I. H. Mixed-Matrix Membranes Composed of Matrimid and MOF-5 for Gas Separations. *J. Membr. Sci.* **2009**, *328*, 165−173.
(18) Chung, T. S.; Jiang, L. Y.; Li, Y.; Kulprathipanja, S. Mixed matrix membranes (MMMs) Comprising Organic Polymers with Dispersed Inorganic Fillers for Gas Separation. *Prog. Polym. Sci.* **2007**, *32*, 483−507.
(19) Ning, X.; Koros, W. J. Carbon Molecular Sieve Membranes Derived from Matrimid® Polyimide for Nitrogen/Methane Separation. *Carbon* **2014**, *66*, 511−522.
(20) Rungta, M.; Xu, L.; Koros, W. J. Carbon Molecular Sieve Dense Film Membranes Derived from Matrimid for Ethylene/Ethane Separation. *Carbon* **2012**, *50*, 1488.
(21) Low, B. T.; Chung, T. S. Carbon Molecular Sieve Membranes Derived from Pseudo- Interpenetrating Polymer Networks for Gas Separation and Carbon Capture. *Carbon* **2011**, *49*, 2104−2112.
(22) Paul, D. R. Creating New Types of Carbon-Based Membranes. *Science* **2012**, *335*, 413.

DOI: 10.1021/acsami.5b04747
ACS Appl. Mater. Interfaces 2015, 7, 18618−18627

(23) Mannan, H. A.; Mukhtar, H.; Murugesan, T.; Nasir, R.; Mohshim, D. F.; Mushtaq, A. Recent Applications of Polymer Blends in Gas Separation Membranes. *Chem. Eng. Technol.* **2013**, *36*, 1838−1846.
(24) Chappell, J.; Lidzey, D. G.; Jukes, P. C.; Higgins, A. M.; Thompson, R. L.; O'Connor, S.; Grizzi, I.; Fletcher, R.; O'Brien, J.; Geoghegan, M.; Jones, R. A. L. Correlating Structure With Fluorescence Emission in Phase-Separated Conjugated-Polymer Blends. *Nat. Mater.* **2003**, *2*, 616−621.
(25) Berggren, M.; Inganas, O.; Gustafsson, G.; Rasmusson, J.; Andersson, M. R.; Hjertberg, T.; Wennerstrom, O. Light-Emitting Diodes with Variable Colors from Polymer Blends. *Nature* **1994**, *372*, 444−446.
(26) Newman, D.; Laredo, E.; Bello, A.; Grillo, A. l.; Feijoo, J. L.; Muller, A. J. Molecular Mobilities in Biodegradable Poly(dl-lactide)/Poly(ε-caprolactone) Blends. *Macromolecules* **2009**, *42*, 5219−5225.
(27) Deimede, V.; Voyiatzis, G. A.; Kallitsis, J. K.; Qingfeng, L.; Bjerrum, N. J. Miscibility Behavior of Polybenzimidazole/Sulfonated Polysulfone Blends for Use in Fuel Cell Applications. *Macromolecules* **2000**, *33*, 7609−7617.
(28) Jung, K. H.; Ferraris, J. P. Preparation and Electrochemical Properties of Carbon Nanofibers Derived from Polybenzimidazole/Polyimide Precursor Blends. *Carbon* **2012**, *50*, 5309.
(29) Robeson, L. *Polymer Blends: A Comprehensive Review*; Hanser Gardner Publications: Cincinnati, OH, 2007.
(30) Zhang, X. H.; Liu, Q. L.; Xiong, Y.; Zhu, A. M.; Chen, Y.; Zhang, Q. G. *J.* Pervaporation Dehydration of Ethyl Acetate/Ethanol/Water Azeotrope using Chitosan/Poly (vinyl pyrrolidone) Blend Membranes. *J. Membr. Sci.* **2009**, *327*, 274−280.
(31) Kumar, R.; Isloor, A. M.; Ismail, A. F.; Rashid, S. A.; Ahmed, A. A. Permeation, Antifouling and Desalination Performance of TiO_2 Nanotube Incorporated PSf/CS Blend Membranes. *Desalination* **2013**, *316*, 76−84.
(32) Hosseini, S. S.; Peng, N.; Chung, T. S. Gas Separation Membranes Developed Through Integration of Polymer Blending and Dual-Layer Hollow Fiber Spinning Process for Hydrogen and Natural Gas Enrichments. *J. Membr. Sci.* **2010**, *349*, 156−166.
(33) Hosseini, S. S.; Teoh, M. M.; Chung, T. S. Hydrogen Separation and Purification in Membranes of Miscible Polymer Blends with Interpenetration Networks. *Polymer* **2008**, *49*, 1594−1603.
(34) Hosseini, S. S.; Chung, T. S. Carbon Membranes from Blends of PBI and Polyimides for N_2/CH_4 and CO_2/CH_4 Separation and Hydrogen Purification. *J. Membr. Sci.* **2009**, *328*, 174−185.
(35) Khan, A. L.; Li, X.; Vankelecom, I. F. J. SPEEK/Matrimid Blend Membranes for CO_2 Separation. *J. Membr. Sci.* **2011**, *380*, 55−62.
(36) Madaeni, S. S.; Mohammadi Nooripour, R.; Vatanpour, V. Preparation and Characterization of Polyimide and Polyethersulfone Blend Membrane for Gas Separation. *Asia-Pac. J. Chem. Eng.* **2012**, *7*, 747−754.
(37) Li, X. G.; Kresse, I.; Springer, J. R.; Nissen, J. R.; Yang, Y. L. Morphology and Gas Permselectivity of Blend Membranes of Polyvinylpyridine with Ethylcellulose. *Polymer* **2001**, *42*, 6859−6869.
(38) Semsarzadeh, M. A.; Ghalei, B. *J.* Characterization and Gas Permeability of Polyurethane and Polyvinyl Acetate Blend Membranes with Polyethylene Oxide−Polypropylene Oxide Block Copolymer. *J. Membr. Sci.* **2012**, *401*−*402*, 97−108.
(39) Fenouillot, F.; Cassagnau, P.; Majeste, J. C. Uneven Distribution of Nanoparticles in Immiscible Fluids: Morphology Development in Polymer Blends. *Polymer* **2009**, *50*, 1333−1350.
(40) Goodarzi, V.; Hassan Jafari, S.; Ali Khonakdar, H.; Ghalei, B.; Mortazavi, M. Assessment of Role of Morphology in Gas Permselectivity of Membranes Based on Polypropylene/ Ethylene Vinyl Acetate/Clay Nanocomposite. *J. Membr. Sci.* **2013**, *445*, 76−87.
(41) Rafailovich, M.; Sokolov, J.; Plainvie, W.; Zhu, S.; Brook, S.; Chu, B. *Compatibilizer for Immiscible Polymer Blends*. U.S. Patent 6,339,121 B1, January 15, 2002.
(42) Chung, H. J.; Kim, J.; Ohno, K.; Composto, R. J. Controlling the Location of Nanoparticles in Polymer Blends by Tuning the Length and End Group of Polymer Brushes. *ACS Macro Lett.* **2012**, *1*, 252−256.
(43) Robeson, L. M. Polymer Blends in Membrane Transport Processes. *Ind. Eng. Chem. Res.* **2010**, *49*, 11859−11865.
(44) Suzuki, T.; Yamada, Y.; Tsujita, Y. Gas Transport Properties of 6FDA-TAPOB Hyper branched Polyimide Membrane. *Polymer* **2004**, *45*, 7167−7171.
(45) Yang, T.; Shi, G. M.; Chung, T. S. Symmetric and Asymmetric Zeolitic Immidazolate Frameworks (Zifs)/ Polybenzimidazole (PBI) Nanocomposite Membranes for Hydrogen Purification at High Temperatures. *Adv. Energy Mater.* **2012**, *2*, 1358−1367.
(46) Omole, I. C.; Miller, S. J.; Koros, W. J. Increased Molecular Weight of a Cross-Linkable Polyimide for Spinning Plasticization Resistant Hollow Fiber Membranes. *Macromolecules* **2008**, *41*, 6367−6375.
(47) Reid, B. D.; Ruiz-Trevino, F. A.; Musselman, I. H.; Balkus, K. J., Jr.; Ferraris, J. P. Gas Permeability Properties of Polysulfone Membranes Containing the Mesoporous Molecular Sieve MCM-41. *Chem. Mater.* **2001**, *13*, 2366−2373.
(48) Koros, W. J.; Fleming, G. K. Membrane-Based Gas Separation. *J. Membr. Sci.* **1993**, *83*, 1−80.
(49) Ghosal, K.; Freeman, B. D. Gas Separation Using Polymer Membranes: An Overview. *Polym. Adv. Technol.* **1994**, *5*, 673−697.
(50) Sadeghi, M.; Semsarzadeh, M. A.; Moadel, H. Enhancement of the Gas Separation Properties of Polybenzimidazole (PBI) Membrane By Incorporation of Silica Nano Particles. *J. Membr. Sci.* **2009**, *331*, 21−30.
(51) Eguchi, H.; Kim, D. J.; Koros, W. J. Chemically Cross-Linkable Polyimide Membranes for Improved Transport Plasticization Resistance for Natural Gas Separation. *Polymer* **2015**, *58*, 121−129.
(52) Panapitiya, N. P.; Wijenayake, S. N.; Huang, Y.; Bushdiecker, D.; Nguyen, D.; Ratanawanate, C.; Kalaw, G. J.; Gilpin, C. J.; Musselman, I. H.; Balkus, K. J., Jr.; Ferraris, J. P. Stabilization of Immiscible Polymer Blends Using Structure Directing Metal Organic Frameworks (MOFs). *Polymer* **2014**, *55*, 2028−2034.
(53) Liu, L.; Li, M. Curing Mechanisms and Kinetic Analysis of DGEBA Cured With a Novel Imidazole Derivative Curing Agent Using DSC Techniques. *J. Appl. Polym. Sci.* **2010**, *117*, 3220−3227.
(54) Cao, Y.; Zhang, J.; Feng, J.; Wu, P. Compatibilization of Immiscible Polymer Blends Using Graphene Oxide Sheets. *ACS Nano* **2011**, *5*, 5920−5927.
(55) Qu, S. Bis(2-methylimidazolium) Terephthalate bis(2-methylimidazole) Tetrahydrate. *Acta Crystallogr., Sect. E: Struct. Rep. Online* **2007**, *63*, 4071.
(56) Li, Y.; Shimizu, H. Compatibilization by Homopolymer: Significant Improvements in the Modulus and Tensile Strength of PPC/PMMA Blends by the Addition of a Small Amount of PVAc. *ACS Appl. Mater. Interfaces* **2009**, *1*, 1650−1655.
(57) Willemse, R. C.; Posthuma de Boer, A.; van Dam, J.; Gotsis, A. D. Co-continuous morphologies in polymer blends: a new model. *Polymer* **1998**, *39*, 5879−5887.
(58) Wang, N.; Yu, J.; Ma, X. Preparation and characterization of thermoplastic starch/PLA blends by one-step reactive extrusion. *Polym. Int.* **2007**, *56*, 1440−1447.
(59) Li, B.; Wan, C. Y.; Zhang, Y.; Ji, J. L. Blends of Poly(2,6-dimethyl-1,4-phenylene oxide)/Polyamide 6 Toughened by Maleated Polystyrene-Based Copolymers: Mechanical Properties, Morphology, and Rheology. *J. Appl. Polym. Sci.* **2010**, *115*, 3385−3392.
(60) http://www.sigmaaldrich.com/catalog/product/aldrich/m50850?lang=en&region=US (Accessed July 30, 2015).

DOI: 10.1021/acsami.5b04747
ACS Appl. Mater. Interfaces 2015, 7, 18618−18627